

SISSA 17/97/EP
 arch-iv/9705392
 May, 1997

A Study of the Day - Night Effect for the Super - Kamiokande Detector: II. Electron Spectrum Deformations and Day - Night Asymmetries

M. Maris ^{a,b)} and S. T. Petcov ^{1 a,c)}

a) Scuola Internazionale Superiore di Studi Avanzati, Trieste, Italy.

b) INFN - Sezione di Pavia, Pavia, Italy.

c) INFN - Sezione di Trieste, Trieste, Italy.

Abstract

Using the results of a high precision calculation of the solar neutrino survival probability for Earth crossing neutrinos in the case of MSW $\nu_e \rightarrow \nu_{\mu(\tau)}$ transition solution of the solar neutrino problem, performed in an earlier study, we derive predictions for the one-year averaged day-night (D-N) asymmetry in the deformations of the e^- - spectrum to be measured with the Super - Kamiokande detector, and for the D-N asymmetry in the energy- integrated one year signal in this detector. The asymmetries are calculated for solar ν_e crossing the Earth mantle only, the core and the (mantle + core) for a large representative set of values of the MSW transition parameters Δm^2 and $\sin^2 2\theta_V$ from the “conservative” MSW solution region obtained by taking into account possible uncertainties in the values of the ^8B and ^7Be neutrino fluxes. The effect of the uncertainties in the value of the bulk matter density and in the chemical composition of the core, on the D-N asymmetry predictions is discussed. It is shown, in particular, that for $\sin^2 2\theta_V \leq 0.013$ the one year average D-N asymmetry for neutrinos crossing the Earth core can be larger than the asymmetry for (only mantle crossing + core crossing) neutrinos by a factor of up to six. Iso - (D-N) asymmetry contours in the $\Delta m^2 - \sin^2 2\theta_V$ plane for the Super - Kamiokande detector are derived in the region $\sin^2 2\theta_V \gtrsim 10^{-4}$ for only mantle crossing, core crossing and (only mantle crossing + core crossing) neutrinos. Our results indicate that the Super - Kamiokande experiment might be able to test the $\sin^2 2\theta_V \leq 0.01$ region of the MSW solution of the solar neutrino problem by performing selective D-N asymmetry measurements.

PACS: 14.60Pq, 26.65, 95.85.Ry

¹Also at: Institute of Nuclear Research and Nuclear Energy, Bulgarian Academy of Sciences, 1784 Sofia, Bulgaria.

1 Introduction

Assuming that the solar neutrinos undergo two - neutrino MSW $\nu_e \rightarrow \nu_{\mu(\tau)}$ transitions in the Sun, and that these transitions are at the origin of the solar neutrino deficit, we have performed in [1] a high - precision calculation of the one - year averaged solar ν_e survival probability for Earth crossing neutrinos, $P_{\oplus}(\nu_e \rightarrow \nu_e)$, reaching the Super - Kamiokande detector. The probability $P_{\oplus}(\nu_e \rightarrow \nu_e)$ was calculated by using, in particular, the elliptical orbit approximation (EOA) to describe the movement of the Earth around the Sun. Results for $P_{\oplus}(\nu_e \rightarrow \nu_e)$ as a function of $E_\nu/\Delta m^2$, E_ν and Δm^2 being the neutrino energy and the neutrino mass squared difference, have been obtained for neutrinos crossing the Earth mantle only, the core, the inner 2/3 of the core and the mantle + core (full night) for a large representative set of values of $\sin^2 2\theta_V$, where θ_V is the neutrino mixing angle in vacuum, from the "conservative" MSW solution region in the $\Delta m^2 - \sin^2 2\theta_V$ plane, derived by taking into account the possible uncertainties in the fluxes of ^8B and ^7Be neutrinos (see, e.g., ref. [2]; for earlier studies see ref. [3]).

We have found in [1], in particular, that for $\sin^2 2\theta_V \leq 0.013$ the one - year averaged D-N asymmetry ² in the probability $P_{\oplus}(\nu_e \rightarrow \nu_e)$ for neutrinos crossing the Earth core can be larger than the asymmetry in the probability for (only mantle crossing + core crossing) neutrinos by a factor of up to six. The enhancement is even larger for neutrinos crossing the inner 2/3 of the core. We have also pointed out to certain subtleties in the calculation of the time averaged ν_e survival probability $P_{\oplus}(\nu_e \rightarrow \nu_e)$ for neutrinos crossing the Earth, which become especially important when $P_{\oplus}(\nu_e \rightarrow \nu_e)$ is computed, for instance, for the core crossing neutrinos only ³.

In the present article we use the results obtained in [1] to investigate the D-N asymmetries in the spectrum of the recoil electrons from the reaction $\nu_e + e^- \rightarrow \nu_e + e^-$ caused by the ^8B neutrinos and in the energy-integrated event rate, to be measured by the Super - Kamiokande experiment. If the solar ^8B neutrinos take part in MSW transitions, the ^8B neutrino spectrum will be deformed by the MSW effect in the Sun, and, for the neutrinos crossing the Earth, by the MSW effect in the Earth. This creates a difference between the (deformed) spectra of neutrinos detected during the day and during the night, which is reflected in the corresponding day and night recoil - e^- spectra. We have computed in [5] the D-N asymmetry in the recoil- e^- spectrum for the same large set of representative values of Δm^2 and $\sin^2 2\theta_V$ from the "conservative" MSW solution region for which the results in [1] have been obtained. The D-N asymmetry in the e^- -spectrum is found for neutrinos crossing the Earth mantle only, the core and the mantle + core. Here we have included only few representative plots showing the magnitude of the D-N asymmetry in the recoil- e^- spectrum to be expected in the case of the two - neutrino MSW $\nu_e \rightarrow \nu_{\mu(\tau)}$ transition solution of the solar neutrino problem. The spectrum asymmetry for the sample of events due to core crossing neutrinos only is strongly enhanced for $\sin^2 2\theta_V \lesssim 0.013$ with respect to the analogous asymmetries for the mantle and for the (only mantle crossing + core crossing) neutrinos. We present also detailed results for the one-year averaged D-N

²A rather complete list of references on the D-N effect is given in ref. [1].

³For further details concerning the technical aspects of the calculations see ref. [1] as well as ref. [4].

asymmetry in the Super - Kamiokande signal for the indicated three samples of events. We find that indeed for $\sin^2 2\theta_V \leq 0.013$ the asymmetry in the sample corresponding to core crossing neutrinos can be larger than the asymmetry in the sample produced by only mantle crossing or by (only mantle crossing + core crossing) neutrinos by a factor of up to six. The dependence of the D-N asymmetries in the three samples on the threshold e^- kinetic energy being used for event selection is also investigated.

We derive iso - (D-N) asymmetry contours in the region of $\sin^2 2\theta_V \gtrsim 10^{-4}$ in the Δm^2 - $\sin^2 2\theta_V$ plane for the signals in the Super - Kamiokande detector produced by neutrinos crossing the mantle, the core and mantle + core. The iso-asymmetry contours for the sample of events due to core crossing neutrinos are obtained for two values of the fraction of electrons, Y_e , in the core: for $Y_e = 0.467$ and 0.500 ⁴.

Our results confirm the conclusion drawn in [1] that the Super - Kamiokande detector might be able to test the $\sin^2 2\theta_V \lesssim 0.01$ region of the MSW solution of the solar neutrino problem.

2 D-N Effect Related Observables

In [1] we have considered four possible groups or samples of solar neutrino events depending on their detection time. We have labeled these samples as *Day*, *Night*, *Core* and *Mantle*, where *Day* and *Night* samples consist of the solar neutrino events detected respectively during the day and during the night, while the other two samples are formed by the events induced by the neutrinos which cross the Earth core (*Core*) and by the neutrinos which does not cross it (*Mantle*). All quantities analyzed in this paper (MSW probability, recoil- e^- spectrum, event rate, asymmetries) refer to one of these samples and correspondingly carry one of the indices D , N , C and M , standing respectively for *Day*, *Night*, *Core*, and *Mantle*. The recoil- e^- spectra associated with the four samples are denoted by $\mathcal{S}^s(T_e)$, where $s = D, N, C, M$, and T_e is the recoil- e^- kinetic energy, while for the event rates we will use the notation \mathcal{R}^s . The symbols $\mathcal{S}_0(T_e)$ and \mathcal{R}_0^s will be used to denote the recoil- e^- spectrum and event rates for massless (“conventionally” behaving) neutrinos, computed using the predictions of a given reference standard solar model. Correspondingly, one has $\mathcal{R}_0^D = \mathcal{R}_0^N = \mathcal{R}_0^C = \mathcal{R}_0^M \equiv \mathcal{R}_0$. The spectra $\mathcal{S}^s(T_e)$, $\mathcal{S}_0(T_e)$ and the event rates \mathcal{R}_0 , \mathcal{R}^s considered in the present article are one year averaged spectra and event rates.

In the present analysis we use the model of ref. [8] with heavy elements diffusion as a reference solar model. As is well known, the shape of the spectrum of ^8B neutrinos, and consequently the shape of the recoil e^- spectrum, is solar model independent. The event rates \mathcal{R}_0 and \mathcal{R}^s depend on the reference solar model prediction for the total flux of ^8B neutrinos. However, the D-N asymmetries we are going to consider, do not depend on the total ^8B neutrino flux and therefore are solar model independent quantities as well.

The spectra $\mathcal{S}_0(T_e)$ and $\mathcal{S}^s(T_e)$ are given by the following standard expressions:

⁴Iso - (D-N) asymmetry contour plots for the full night (i.e., mantle + core) signal for the Super - Kamiokande detector for one value of Y_e have been obtained in refs. [6, 7].

$$\mathcal{S}_0(T_e) = \Phi_B \int_{T_e(1+\frac{m_e}{2T_e})} dE_\nu n(E_\nu) \frac{d\sigma_{\nu_e}(T_e, E_\nu)}{dT_e}, \quad (1)$$

and

$$\begin{aligned} \mathcal{S}^s(T_e) = \Phi_B \int_{T_e(1+\frac{m_e}{2T_e})} dE_\nu n u(E_\nu) & \left[\frac{d\sigma_{\nu_e}(T_e, E_\nu)}{dT_e} P_\oplus^s(\nu_e \rightarrow \nu_e) + \right. \\ & \left. + \frac{d\sigma_{\nu_\mu}(T_e, E_\nu)}{dT_e} (1 - P_\oplus^s(\nu_e \rightarrow \nu_e)) \right]. \end{aligned} \quad (2)$$

Here Φ_B is the total ${}^8\text{B}$ neutrino flux, E_ν is the incoming ${}^8\text{B}$ neutrino energy, m_e is the electron mass, $n(E_\nu)$ is the normalized to one ${}^8\text{B}$ neutrino spectrum [10], $P_\oplus^s(\nu_e \rightarrow \nu_e)$ is the one year averaged solar ν_e survival probability for *Day*, *Night*, *Core*, and *Mantle* samples, and $d\sigma_{\nu_e(\nu_\mu)}(T_e, E_\nu)/dT_e$ is the differential ν_e ($\nu_\mu(\tau)$) - e^- elastic scattering cross section [9]. For the corresponding energy integrated event rates we have:

$$\begin{aligned} \mathcal{R}_0(T_{e,th}) &= \int_{T_{e,th}} dT_e \mathcal{S}_0(T_e), \\ \mathcal{R}^s(T_{e,th}) &= \int_{T_{e,th}} dT_e \mathcal{S}^s(T_e), \end{aligned} \quad (3)$$

where $T_{e,th}$ is the recoil- e^- kinetic energy threshold of the Super - Kamiokande detector. The results reported in the present study are obtained for $T_{e,th} = 5$ MeV.

In this article we present results for three observables relevant to D-N effect which can be measured with the Super - Kamiokande detector. The first is the distortion of the recoil- e^- spectrum due to the MSW effect for the four different event samples:

$$\mathcal{N}^s(T_e) = \frac{\mathcal{S}^s(T_e)}{\mathcal{S}_0(T_e)}, \quad s = D, N, C, M. \quad (4)$$

In the absence of the MSW effect, or in the case of energy - independent (constant) reduction of the ${}^8\text{B}$ ν_e flux at $E_\nu \geq 5$ MeV, we would have $\mathcal{N}^s(T_e) = \text{const.}$ The spectrum ratio $\mathcal{N}^s(T_e)$ shows the magnitude and the shape of the e^- spectrum deformations (with respect to the standard spectrum) due to the MSW effect taking place in the Sun only, as well as in the Sun and in the Earth mantle, core and mantle + core.

The second observable we consider is the D-N asymmetry in the recoil- e^- spectrum for the three solar neutrino event samples, associated with the MSW effect in the Earth:

$$\mathcal{A}_{D-N}^s(T_e) = 2 \frac{\mathcal{S}^s(T_e) - \mathcal{S}^D(T_e)}{\mathcal{S}^s(T_e) + \mathcal{S}^D(T_e)}, \quad s = N, C, M. \quad (5)$$

The third observable is the energy integrated event rate asymmetry:

$$A_{D-N}^s(T_{e,th}) = 2 \frac{\mathcal{R}^s - \mathcal{R}^D}{\mathcal{R}^s + \mathcal{R}^D}, \quad s = N, C, M. \quad (6)$$

Both these observables are solar model independent.

The observation of a nonzero D-N asymmetry $A_{D-N}^s \neq 0$ and/or $\mathcal{A}_{D-N}^s(T_e) \neq 0$ would be a very strong evidence (if not a proof) that solar neutrinos undergo MSW transitions. If, on the other hand, no statistically significant D-N effect would be found within the accuracy of the measurements to be reached in the Super - Kamiokande experiment, a large region of the MSW solution values of the parameters Δm^2 and $\sin^2 2\theta_V$ would be excluded.

The one year averaged spectrum ratio $\mathcal{N}^s(T_e)$ $s = D, N, C, M$, and the spectrum and event rate D-N asymmetries $\mathcal{A}_{D-N}^s(T_e)$ and A_{D-N}^s , $s = N, C, M$, for the Super - Kamiokande detector have been calculated for 36 pairs of values of Δm^2 and $\sin^2 2\theta_V$ distributed evenly in the ‘‘conservative’’ MSW solution region (see [1, 2]). These values together with the corresponding results for $A_{D-N}^{N,C,M}$ as well as for the ratio A_{D-N}^C/A_{D-N}^N , are given in Table II. We present here graphically in Figs. 2.1 - 2.12 only some of the results obtained for $\mathcal{N}^s(T_e)$ and $\mathcal{A}_{D-N}^s(T_e)$ (see ref. [5] for a more complete set of figures). Figs. 3a - 3c contain plots of contours in the $\Delta m^2 - \sin^2 2\theta_V$ plane, corresponding to fixed values of the event rate asymmetries $A_{D-N}^{N,C,M}$ (iso - (D-N) asymmetry contours) in the region of $\sin^2 2\theta_V \gtrsim 10^{-4}$.

3 Earth Model Uncertainties

The Earth electron number density $n_e(x)$, which enters in the calculations of the D-N effect, is proportional to the product $Y_e(x)\rho(x)$, where $Y_e(x)$ is the number of electrons per nucleon and $\rho(x)$ is the matter density at distance x from the center of the Earth. While both $Y_e(x)$ and $\rho(x)$ are functions of the local chemical composition, $\rho(x)$ is also a function of the phase (solid, liquid, crystal) of the state of matter. The phase can be inferred from measurements of the propagation of s and p seismic waves in the Earth. These measurements permitted to reconstruct the approximate onion-like structure of the Earth’s interior, each strata being characterized by materials which are in definite phases having definite chemical composition.

As already was mentioned, the two main components of the Earth structure are the core and the mantle. Both of them are characterized by a strong differentiation in both the chemical composition and the state phases. The chemical composition of the core and of the mantle cannot be inferred from the seismic data only. It is deduced by comparing

results from laboratory experiments, the seismic data, and the predictions of models (for further details see, e.g., refs. [11, 12, 13, 14]). In laboratory experiments one studies the chemical and physical behavior of the materials at the Earth interior conditions, where the temperature and the pressure reach values of the order of few $\times 10^3$ K and few $\times 10^{11}$ Pa, to obtain a quantitative measure of the correlation between pressure, density, composition and the sound velocity. The interior Earth conditions are reproduced by studying samples subjected to high pressures and high temperatures in either a diamond-anvil-cell or in shock-wave experiments. One of the major aims of these experiments is to produce a realistic model for the Earth's chemical composition. Since it is supposed that the Earth formed as a result of gravitational accretion of planetesimals which are believed to be also the source of meteorites, it is suggested that the chemical composition of the Earth interior resembles to a large extent that of meteorites. The mantle is expected to have a composition similar to the composition of the *chondritic* meteorites consisting mainly of $(\text{Mg,Fe})\text{SiO}_3$. The core composition is supposed to be similar to that of the iron meteorites, i.e., an alloy of Fe and Ni with at most 10% (by weight) of Ni. However, while the seismic constraints are compatible with the chemical composition of the mantle thus deduced, they are not compatible with the indicated core composition. The outer core has to be an alloy of iron with 10% of some lighter element such as O, S, Si. The presence of light elements in the outer core may be due to the drag of materials from the mantle toward the Earth center driven by the gravitational settling of the molten iron during the inner Earth differentiation. It may also be due to chemical instabilities caused by strong chemical in-equilibrium at the core/mantle interface, which can produce chemical reactions and/or diffusion enriching the core with light elements and the mantle with heavy ones.

Calculations based on the various possible chemical compositions of the two major Earth substructures show that $Y_e \approx (0.49 - 0.50)$ for the mantle, while for the core $Y_e \approx (0.46 - 0.48)$. At the same time the bulk matter density of the core ρ can be inferred from the seismological data with an uncertainty which is estimated to be between 5% and 10%, the latter value representing a conservative upper limit. Thus, the uncertainty in the knowledge of ρ is the major source of uncertainty in the quantity $Y_e\rho$ for the core.

Other source of uncertainty in the Earth model are the thickness of the core/mantle boundary region and the value of the core radius. Both of them are strongly constrained by seismological data and the corresponding uncertainties do not exceed ~ 10 km. The uncertainties they introduce in the magnitude of the D-N asymmetries are negligible because the corresponding residence time associated with them is exceedingly small. For the same reason the detailed structure of the core-mantle boundary region, more specifically, the change of density in this region (continuous versus discontinuous) is not important for a calculation of the D-N effect with a precision of (1 - 2)% [15].

4 D-N Effect and the Recoil- e^- Spectrum

In Figs. 1 and 2.1 - 2.12 we show examples respectively of the predicted recoil - e^- spectrum, $\mathcal{S}_0(T_e)$, the spectrum distortions due to the MSW effect in the Earth and/or in the Sun,

$\mathcal{S}^s(T_e)$, and of the ratio of spectra, $\mathcal{N}^s(T_e)$, and the D-N asymmetries in the spectrum for the different event samples, $\mathcal{A}_{D-N}^s(T_e)$. This is done for representative subset of neutrino parameters Δm^2 and $\sin^2 2\theta_V$, chosen from the set listed in Table I. The “presence” of the Earth effect in the e^- -spectrum is better illustrated by the ratio $\mathcal{N}^s(T_e)$ and by the asymmetries $\mathcal{A}_{D-N}^s(T_e)$ than by the spectra $\mathcal{S}^s(T_e)$. For this reason we report as an example in Fig. 1 only one set of spectra $\mathcal{S}^s(T_e)$ calculated for $\sin^2 2\theta_V = 0.01$, $\Delta m^2 = 5 \times 10^{-5} \text{ eV}^2$ and $Y_e = 0.467$. The *upper solid* line in Fig. 1 is the standard e^- -spectrum $\mathcal{S}_0(T_e)$, while $\mathcal{S}^D(T_e)$, $\mathcal{S}^N(T_e)$, $\mathcal{S}^C(T_e)$ and $\mathcal{S}^D(T_e)$ are represented respectively by the *long - dashed*, the *short - dashed*, the *lower solid* and the *dotted* lines. It should be noted that since in the Super - Kamiokande experiment the background rejection is achieved, in particular, through a cut in the angle between the scattered electron momentum direction and the Sun’s direction, the measured spectra (and their related distortions and D-N asymmetries) depend, in general, on the cut being used. For the Super - Kamiokande detector e^- kinetic energy threshold of 5 MeV, however, the effect of the angular cut on the spectra of interest, as can be shown, is negligible ⁵.

The e^- -spectrum distortions $\mathcal{N}^s(T_e)$ and D-N asymmetries $\mathcal{A}_{D-N}^s(T_e)$ depicted in Figs. 2.1 - 2.12 (the upper and the lower frame of each figure) were computed for $Y_e = 0.467$. The enhancement of the spectrum distortions and of the D-N asymmetry in the *Core* sample is clearly seen, especially for $\sin^2 2\theta_V \lesssim 0.013$. The magnitude of the Earth effect in the spectrum is sensitive to the value of Δm^2 , since spectral signatures such as kinks, knees and peaks (that may be associated with similar features in the the corresponding solar ν_e survival probabilities reported in ref. [1]) change their position in the kinetic energy window when Δm^2 changes (see Figs. 2.1, 2.2 and 2.3 as well as Figs. 2.4, 2.5 and 2.6).

Both the spectra $\mathcal{S}^s(T_e)$, the spectral distortions $\mathcal{N}^s(T_e)$ shown in Figs. 1 and 2.1 - 2.12 and the event rates given in Table I are normalized to the event rate predicted for standard neutrinos in the reference solar model [8]. That means that if the neutrino parameters belong to the “conservative” MSW solution regions but lie outside the solution regions obtained within the reference solar model, one should re-scale $\mathcal{S}^s(T_e)$, $\mathcal{N}^s(T_e)$ and the event rates in Table I, multiplying them by the factor $f_B = \Phi_B^{MSW} / \Phi_B$, where Φ_B^{MSW} is the ^8B neutrino flux which was used in the MSW analysis of the solar neutrino data and for which the corresponding solution region was obtained (see refs. [2, 3] for details). We give in Table I the values of the factor f_B associated with each pair of values of Δm^2 and $\sin^2 2\theta_V$, for which the event rates listed in Table I and the quantities $\mathcal{S}^s(T_e)$ and $\mathcal{N}^s(T_e)$ depicted in Figs. 1 and 2.1 - 2.12 have been calculated.

The differences between the *Day* and the *Night (Mantle)* sample e^- spectra are hardly observable, as Figs. 2.1 - 2.12 indicate. However, as it follows from Figs. 2.4, 2.5, 2.7, 2.10 and 2.12, the *Core* sample spectrum can differ significantly (both in shape and magnitude) from the *Day* sample spectrum. For $\sin^2 2\theta_V \geq 0.008$ and for a large number of values of Δm^2 from the “conservative” MSW solution region the *Core* sample D-N asymmetry in the spectrum $\mathcal{A}_{D-N}^C(T_e)$ is bigger than 10% at least in a significant subinterval of values of T_e from the relevant interval (5 - 14) MeV. In certain cases the asymmetry $\mathcal{A}_{D-N}^C(T_e)$ can

⁵The effect of the indicated angular cut on the spectra of interest becomes important for $T_e \lesssim 4$ MeV.

reach values of 20% - 30% (Figs. 2.5, 2.6 and 2.8) and even 50% (Fig. 2.10). At the same time, for certain pairs of values of Δm^2 and $\sin^2 2\theta_V$, $\mathcal{A}_{D-N}^C(T_e)$ is rather small in the whole e^- kinetic energy interval of interest. For instance, if $\Delta m^2 = 4 \times 10^{-5} \text{ eV}^2$ ($5 \times 10^{-5} \text{ eV}^2$) and $\sin^2 2\theta_V = 0.3$ (0.7) we have $\mathcal{A}_{D-N}^C(T_e) \leq 6\%$ (7.5%). In any case, the measurement of the *Core* sample e^- -spectrum as well as of the asymmetry $\mathcal{A}_{D-N}^C(T_e)$ can allow to obtain additional constraints on the MSW transition parameters Δm^2 and $\sin^2 2\theta_V$.

Finally, we would like to note that, we have performed a comparison between the spectra and the related spectrum distortions and D-N asymmetries, computed for $Y_e = 0.467$ and for $Y_e = 0.50$. The differences are relatively small if one takes into account the precision in the measurement of the recoil- e^- spectrum, which is expected to be reached in the Super - Kamiokande experiment. The ratio $\mathcal{N}^s(T_e)$ and the D-N asymmetries $\mathcal{A}_{D-N}^s(T_e)$ computed for $Y_e = 0.50$ and the set of neutrino parameters $\sin^2 2\theta_V$ and Δm^2 given in Table I can be found in ref. [5].

5 Energy-Integrated D-N Asymmetries

Figures 3a, 3b and 3c represent the iso-(D-N) asymmetry contour plots for the *Night*, *Core* and *Mantle* samples. Shown are also the “conservative” regions of the two MSW solutions of the solar neutrino problem (dashed lines) as well as the solution regions obtained in the reference solar model [8] (dotted lines). The iso-asymmetry lines in the figures correspond to $A_{D-N}^{N,C,M} = -2\%$, -1% , $+1\%$, $+2.5\%$, $+10\%$, $+20\%$, $+40\%$, $+60\%$, $+80\%$, $+90\%$, $+100\%$. The iso-(D-N) asymmetry contours for the *Night* and *Core* samples shown in Figs. 3a and 3b have been obtained both for $Y_e = 0.467$ (solid lines) and for $Y_e = 0.5$ (dash-dotted lines). Since the Earth effect depends on the quantity $Y_e \rho$, the case of $Y_e = 0.500$ and a given matter density distribution in the core is equivalent to the case of $Y_e = 0.467$ and a core matter density which is uniformly increased by 7%. For given Δm^2 and $\sin^2 2\theta_V$ the differences between A_{D-N}^N or A_{D-N}^M and A_{D-N}^C are largest in the region of the nonadiabatic (NA) or small mixing angle solution.

The magnitude of the D-N asymmetry in the region of the large mixing angle adiabatic (AD) solution does not change significantly with the change of the sample. As we have already pointed out in ref. [1], although the *Core* enhancement of the D-N effect at large mixing angles is noticeable, it is not dramatic. The asymmetry A_{D-N}^N (A_{D-N}^C) is predicted to vary approximately between 0.01 and 0.35 (0.42) in the “conservative” region of the AD solution. Since the neutrino transitions in the mantle are the dominant source of the Earth effect in this case, the same conclusion should be valid even if the data are taken over a period which represents a fraction of the year.

In contrast, in the NA solution region the D-N asymmetry in the *Core* sample is enhanced by a factor of up to six. The reduction in statistics for this sample increases the statistical error by a factor of 2.65. Therefore the effective enhancement is by about a factor of 2.3, which is quite significant. The D-N asymmetry for the *Core* sample is greater than 0.01 in absolute value in most of the “conservative” NA solution region (see Fig. 3b). In the NA solution region derived in the reference solar model A_{D-N}^C takes values in the

interval (0.025 - 0.20). Our results show that the A_{D-N}^C does not exceed approximately 0.30 in the region of the NA solution. It is interesting to note also that a negative Earth effect larger in absolute value than 1% is predicted for the core sample for most of the values of the parameters from the “conservative” NA solution region. Note that the +10% effect line crosses only marginally the “conservative” NA solution region in the case of the *Night* sample (Fig. 3a). A comparison between Fig. 3a and Fig. 3b indicates that the *Core* selection is a very effective method of enhancing the D-N asymmetry in the data sample despite the loss of statistics.

The difference between the values of the *Core* sample asymmetry A_{D-N}^C calculated for $Y_e = 0.467$ and for $Y_e = 0.5$ depends very strongly on the values of Δm^2 and $\sin^2 2\theta_V$. For most of the values of Δm^2 and $\sin^2 2\theta_V$ from the “conservative” regions of the two MSW solutions (see Fig. 3b and Table II) this difference does not exceed 0.01 in absolute value. However, for certain $\sin^2 2\theta_V$ and specific values of Δm^2 from the NA solution region it can be larger than 0.02 in absolute value. As Table II illustrates, for $\sin^2 2\theta_V = 0.006; 0.008; 0.01; 0.013$, A_{D-N}^C can change respectively by -0.022; -0.047; -0.03; +0.026 when Y_e is changed from 0.467 to 0.500. This change in the region of the AD solution is typically smaller than 0.02 in absolute value, except for $\sin^2 2\theta_V \cong 0.56$ when the change can be as large as by (-0.059). The values of the D-N asymmetry for the *Night* sample calculated for the two indicated values of Y_e typically do not differ by more 0.01 in absolute value. The only exception is the case of $\sin^2 2\theta_V \cong 0.56$ for which the difference can be considerably larger (can be equal to (-0.039), for instance).

The D-N asymmetry in the *Mantle* sample is smaller than 10% in the “conservative” NA solution region; in the AD solution region it can be as large as 35%.

Because of the large differences between the core and the mantle structures, the *Mantle* and *Core* subsamples provide two independent measurements of the D-N effect. These can be combined to constrain better the neutrino parameters Δm^2 and $\sin^2 2\theta_V$, utilizing the full statistics of the *Night* sample. Since the core enhancement is larger at small mixing angles, the NA solution region can be more effectively constrained than the AD solution region by the combined use of the D-N asymmetry values in the *Core* and *Mantle* samples. In the NA solution region, the iso-asymmetry contour lines for the *Mantle* and the *Core* samples cross each other nearly perpendicularly. Therefore if $\sin^2 2\theta_V \gtrsim 8 \times 10^{-3}$ and $3.5 \times 10^{-6} \text{ eV}^2 \lesssim \Delta m^2 \lesssim 6 \times 10^{-6} \text{ eV}^2$ it should be possible to reduce considerably the allowed NA region by just combining the experimental results for A_{D-N}^C and A_{D-N}^M . Outside this region the D-N effect can be detectable only in the *Core* sample for $\sin^2 2\theta_V \gtrsim 5 \times 10^{-3}$. If, for instance, a +10% D-N asymmetry will be detected in the *Core* sample and no D-N asymmetry will be observed in the *Mantle* sample, the NA solution region would be restricted to a narrow band along the +10% line, limited approximately by $6 \times 10^{-3} \lesssim \sin^2 2\theta_V \lesssim 8 \times 10^{-3}$ and $5 \times 10^{-6} \text{ eV}^2 \lesssim \Delta m^2 \lesssim 10^{-5} \text{ eV}^2$. For $\sin^2 2\theta_V \lesssim 5 \times 10^{-3}$ the Earth effect is negative and it does not exceed 3.5% in absolute value. A negative D-N asymmetry larger than 0.01 in absolute value is possible both for the *Core* and the *Mantle* samples in a small region of values of the parameters centered around $\sin^2 2\theta_V \approx 3 \times 10^{-3}$ and $\Delta m^2 \approx 3 \times 10^{-6} \text{ eV}^2$. For the allowed values of Δm^2 and $\sin^2 2\theta_V$ from the NA region derived within the reference solar model [8], the Earth effect is positive both for the core and the mantle

samples. However, A_{D-N}^C can be negative for values of Δm^2 and $\sin^2 2\theta_V$ from the “conservative” NA solution region. If a negative Earth effect with $|A_{D-N}^C| \geq 0.02$ will be detected, the NA solution will be restricted to the narrow region determined by the inequalities $1.3 \times 10^{-3} \lesssim \sin^2 2\theta_V \lesssim 3 \times 10^{-3}$ and $5 \times 10^{-6} \text{ eV}^2 \lesssim \Delta m^2 \lesssim 7.5 \times 10^{-6} \text{ eV}^2$.

Using the mean event rate solar neutrino data provided by the different solar neutrino detectors and the measurements of the D-N asymmetry in the Super-Kamiokande experiment can allow to obtain information not only about the parameters Δm^2 and $\sin^2 2\theta_V$, but also about the value of the ^8B neutrino flux provided the solar neutrinos undergo MSW transitions in the Sun and in the Earth. Indeed, a change of Φ_B shifts the region of the NA solution, obtained for a given value of Φ_B , along the $\sin^2 2\theta_V$ axis, leaving the region’s shape and dimensions essentially unchanged (to less extent a similar behavior is exhibited by the large mixing angle solution region). The iso - (D-N) asymmetry contours cross nearly vertically the “conservative” NA solution region, derived by varying Φ_B and using the predictions of the reference solar model [8] for the other solar neutrino flux components. Thus, the measurement of the D-N asymmetry can allow to select an MSW solution of the solar neutrino problem which corresponds to a given value of Φ_B . For example, a +10% D-N effect in the NA region would correspond to a value of Φ_B expected in the reference solar model [8], while the absence of a positive D-N effect at 1% – 2% level, would indicate either that the MSW effect does not take place or that the ^8B neutrino flux is smaller than the flux in the reference model [8]. The D-N asymmetry is independent on the ^8B neutrino flux, and the MSW probability $P_{\oplus}^s(\nu_e \rightarrow \nu_e)$ varies very little when calculated in different standard solar models which are compatible with the existing observational constraints ⁶. Thus, the measurement of the D-N asymmetry allows to determine $\sin^2 2\theta_V$ and Δm^2 essentially in a solar model independent way. The uncertainties in the iso - (D-N) asymmetry contours associated with the Earth model being used in the calculations are smaller than the uncertainties in the MSW solution regions associated with the spread in the solar model predictions for the value of the ^8B neutrino flux.

We have studied also the dependence of the asymmetries $A_{D-N}^s(T_{e,th})$ for $Y_e = 0.467$ on the value of the threshold energy $T_{e,th}$ being used in the event selection, by performing a calculation of A_{D-N}^s for $T_{e,th} = 7.5 \text{ MeV}$ as well. The results of this analysis are presented in Table III. We have found that in the cases of the *Night* and *Mantle* samples one can have $|A_{D-N}^{N(M)}(7.5 \text{ MeV}) - A_{D-N}^{N(M)}(5.0 \text{ MeV})| \geq 0.01$ only for $\sin^2 2\theta_V \gtrsim 0.013$, where $A_{D-N}^s(7.5 \text{ MeV})$ and $A_{D-N}^s(5.0 \text{ MeV})$ are the values of the asymmetries for $T_{e,th} = 7.5 \text{ MeV}$ and $T_{e,th} = 5.0 \text{ MeV}$. Moreover, when the indicated difference is larger than 0.01, it is always positive, i.e., we have $A_{D-N}^{N(M)}(7.5 \text{ MeV}) > A_{D-N}^{N(M)}(5.0 \text{ MeV})$. This is due mainly to the fact that the event rate \mathcal{R}^D decreases with the increase of $T_{e,th}$. It should be emphasized, however, that for the values of $\sin^2 2\theta_V \gtrsim 0.013$ and Δm^2 from Table III, for which the calculations with $T_{e,th} = 7.5 \text{ MeV}$ have been done, one has typically $|A_{D-N}^{N(M)}(7.5 \text{ MeV}) - A_{D-N}^{N(M)}(5.0 \text{ MeV})| \sim (0.01 - 0.02)$. The difference between the

⁶The solar ν_e survival probability depends in the case of interest, as is well known, on the electron number density distribution in the Sun. All contemporary solar models compatible with the helioseismological observations predict very similar electron number density distributions in the Sun.

$T_{e,th} = 7.5$ MeV and the $T_{e,th} = 5.0$ MeV asymmetries for the *Night (Mantle)* sample reaches the maximal value of 0.051 (0.038) for $\sin^2 2\theta_V \cong 0.56$ and $\Delta m^2 \cong 10^{-5} eV^2$ ($f_B = 1.5$).

As it follows from Table III, the dependence of the *Core* sample asymmetry A_{D-N}^C on $T_{e,th}$ is much stronger and more complicated. For $\sin^2 2\theta_V \geq 0.006$ one typically has $|A_{D-N}^C(7.5 \text{ MeV}) - A_{D-N}^C(5.0 \text{ MeV})| \geq 0.02$. This difference can take the values of -0.046, -0.076, -0.117 for $\sin^2 2\theta_V \cong 0.008, 0.01, 0.013$, i.e., the change of $T_{e,th}$ from 5 MeV to 7.5 MeV can decrease considerably the asymmetry A_{D-N}^C . This is not a general rule, however: for $\sin^2 2\theta_V \cong 0.008$, for instance, A_{D-N}^C increases by 0.034 when $T_{e,th}$ is raised to 7.5 MeV if $\Delta m^2 \cong 10^{-5} eV^2$, and decreases by 0.046 if $\Delta m^2 \cong 5 \times 10^{-6} eV^2$. The indicated dependence can be exploited to obtain better constraints on the two neutrino transition parameters Δm^2 and $\sin^2 2\theta_V$ as well as on the value of the ^8B neutrino flux if the existence of the D-N effect will be established.

6 Conclusions

Assuming that the solar neutrinos undergo two-neutrino MSW $\nu_e \rightarrow \nu_{\mu(\tau)}$ transitions which are at the origin of the solar neutrino problem and using the results of a high precision calculation of the MSW solar ν_e survival probability performed in ref. [1], we have derived in the present article detailed predictions for several D-N effect related observables for the Super-Kamiokande detector. The observables we have studied here are: i) the shape of the recoil- e^- spectrum $\mathcal{S}^s(T_e)$, and the ratio $\mathcal{N}^s(T_e) = \mathcal{S}^s(T_e)/\mathcal{S}_0(T_e)$, $\mathcal{S}_0(T_e)$ being the standard spectrum in the case of ‘‘conventionally’’ behaving (on the way to the Earth and the detector) solar ^8B neutrinos, ii) the D-N asymmetry in the spectrum, $\mathcal{A}_{D-N}^s(T_e)$, and iii) the energy-integrated D-N asymmetry, A_{D-N}^s . The observables $\mathcal{S}^s(T_e)$ ($\mathcal{N}^s(T_e)$), $\mathcal{A}_{D-N}^s(T_e)$ and A_{D-N}^s have been calculated for three different samples of events produced respectively by solar neutrinos which cross the Earth mantle only ($s = M$), the Earth core ($s = C$) and the mantle only + the core (full night, $s = N$). The e^- -spectrum has been derived also for the sample of events detected during the day ($s = D$). Obviously, $\mathcal{S}^D(T_e)$ ($\mathcal{N}^D(T_e)$) is sensitive to the MSW effect in the Sun, while $\mathcal{S}^s(T_e)$ ($\mathcal{N}^s(T_e)$), $\mathcal{A}_{D-N}^s(T_e)$ and A_{D-N}^s , $s = N, C, M$, depend both on the solar neutrino transitions in the Sun and in the Earth.

All quantities for which we have obtained predictions, $\mathcal{S}^s(T_e)$ ($\mathcal{N}^s(T_e)$), $\mathcal{A}_{D-N}^s(T_e)$ and A_{D-N}^s , are one year averaged. The energy-integrated asymmetries A_{D-N}^s have been calculated for e^- kinetic energy threshold of $T_{e,th} = 5 \text{ MeV}$. The calculation of the *Mantle (Core)* sample observables has been performed for $Y_e = 0.50$ (0.467). We have studied the dependence of the predictions for the *Core* sample observables on the uncertainties in the chemical composition and in the value of the bulk matter density of the Earth core. The dependence of the asymmetries A_{D-N}^N , A_{D-N}^C and A_{D-N}^M on the threshold energy $T_{e,th}$ being used for the event selection was also investigated by comparing the values of the asymmetries calculated for $T_{e,th} = 5.0 \text{ MeV}$ and for $T_{e,th} = 7.5 \text{ MeV}$ (Table III). Iso - (D-N) asymmetry contour plots for the *Night*, *Core* and *Mantle* samples have been obtained for $\sin^2 2\theta_V \gtrsim 10^{-4}$, i.e., in the ‘‘conservative’’ region of the MSW solution of the solar neutrino

problem, derived by varying the ^8B and ^7Be neutrino fluxes (see refs. [2, 3]).

The results of the present study can be summarized as follows.

1. The *Core* sample D-N asymmetry A_{D-N}^C can be strongly enhanced with respect to the *Night* and *Mantle* sample asymmetries A_{D-N}^N and A_{D-N}^M . Such an enhancement takes place in the region of the NA solution of the solar neutrino problem, i.e., for $\sin^2 2\theta_V \leq 0.013$: it can be as large as by a factor of six. In the region of the AD solution A_{D-N}^C is larger than A_{D-N}^N by a factor which does not exceed 1.5.

2. The asymmetry A_{D-N}^C is greater than 1% in absolute value in most of the “conservative” NA solution region; it does not exceed 30% in this region (Fig. 3b). For certain Δm^2 and $\sin^2 2\theta_V$ we have $A_{D-N}^C = -(2.0 - 3.5)\%$. In the “conservative” region of the AD solution A_{D-N}^C is predicted to lie in the interval (1.0 - 42.0)%.

The *Night* sample asymmetry A_{D-N}^N takes values between 1% and 10% (1% and 35%) in the NA (AD) solution region (Fig. 3a). One has $A_{D-N}^N \geq 1.0\%$ only in a small subregion of the “conservative” NA solution region (this subregion constitutes a part of the reference solar model [8] solution region). Similar conclusions are valid for the *Mantle* sample asymmetry A_{D-N}^M (Fig. 3c).

3. The difference between the values of A_{D-N}^C calculated for $Y_e = 0.467$ and for $Y_e = 0.50$ depends very strongly on the values of Δm^2 and $\sin^2 2\theta_V$ (Fig. 3b and Table II). Although for most Δm^2 and $\sin^2 2\theta_V$ from the “conservative” MSW solution regions this difference does not exceed 0.01 in absolute value, for certain combinations of values of $\sin^2 2\theta_V$ and Δm^2 it can be as large as -0.047 (-0.059) in the NA (AD) solution region. The analogous difference for the *Night* sample asymmetry A_{D-N}^N is typically smaller than (0.01 - 0.02) in absolute value, one exception being the case of $\sin^2 2\theta_V \sim 0.56$ when it can reach the value of -0.039.

4. Raising the threshold energy $T_{e,th}$ can change considerably the value of the *Core* sample asymmetry A_{D-N}^C : depending on the values of $\sin^2 2\theta_V$ and Δm^2 it can either increase or decrease A_{D-N}^C (Table III). The dependence of A_{D-N}^N and A_{D-N}^M on $T_{e,th}$ is weaker. The sensitivity of A_{D-N}^C to the value of $T_{e,th}$ can be used to better constrain the values of $\sin^2 2\theta_V$ and Δm^2 if the D-N effect will be observed.

5. The measurement of the *Core* and *Mantle* sample asymmetries A_{D-N}^C and A_{D-N}^M can be used not only to constrain the allowed regions of values of the parameters Δm^2 and $\sin^2 2\theta_V$, but also to obtain information about the value of the ^8B neutrino flux.

6. The *Core* sample spectrum $\mathcal{S}^C(T_e)$ can differ significantly (both in shape and magnitude) from the *Day* sample spectrum, $\mathcal{S}^D(T_e)$. In certain cases the *Core* sample D-N asymmetry in the spectrum $\mathcal{A}_{D-N}^C(T_e)$ can reach values of (20 - 30)% (Figs. 2.5, 2.6, 2.8) and even 50% (Fig. 2.10).

The above results indicate that the Super-Kamiokande experiment might be able to test, in particular, the $\sin^2 2\theta_V \leq 0.01$ region of the MSW solution of the solar neutrino problem by performing selective D-N asymmetry measurements. In the case of observation of a nonzero D-N effect, these measurements can allow to determine the value of the ^8B neutrino flux which is compatible with the hypothesis that the solar ν_e undergo two-neutrino MSW $\nu_e \rightarrow \nu_{\mu(\tau)}$ transitions.

7 Acknowledgments

We are indebted to the ICARUS group of the University of Pavia and INFN, Sezione di Pavia, and especially to Prof. E. Calligarich, for allowing the use of their computing facilities for the present study. S.T.P is grateful to A. Duda for useful discussions and to B. Machet and the other members of L.P.T.H.E., Université de Paris 7, where part of the work for the present study has been done, for the kind hospitality extended to him during his visit. M.M. wishes to thank Prof. A. Piazzoli for constant interest in the work and support and the International School for Advanced Studies, Trieste, where most of the work for this study has been done, for financial support. We would like to thank also E. Lisi for informing us about the publication [7] as well as for correspondence. The work of S.T.P. was supported in part by the EEC grant ERBFMRXCT960090 and by Grant PH-510 from the Bulgarian Science Foundation.

References

- [1] Q.Y. Liu, M. Maris and S.T. Petcov, Preprint SISSA 16/97/EP, January 1997 (hep-ph/9702361).
- [2] S.T. Petcov, Nucl. Phys. B (Proc. Suppl.) **43**, 12 (1995); P.I. Krastev and S.T. Petcov, reported by S.T. Petcov at the “Neutrino ’96” Int. Conf. on Neutrino Physics and Astrophysics, 13 - 19 June, 1996, Helsinki, Finland (to be published in the Proceedings of the Conference).
- [3] P.I. Krastev and A.Yu. Smirnov, Phys. Lett. **B338**, 282 (1994); V Berezinsky, G. Fiorentini and M. Lissia, *ibid.* **B341**, 38 (1994); N. Hata and P. Langacker, Phys. Rev. D **52**, 420 (1995).
- [4] M. Maris, Talk given at the *Fourth International Solar Neutrino Conference*, April 8 - 11, 1997, Heidelberg, Germany (to be published in the Proceedings of the Conference).
- [5] M. Maris and S.T. Petcov, E-archive report hep-ph/9703207, February 1997.
- [6] P.I. Krastev, E-archive report hep-ph/9610339, October 1996.
- [7] E. Lisi and D. Montanino, E-archive report hep-ph/9702343, February 1997.
- [8] J.N. Bahcall and M.H. Pinsonneault, Rev. Mod. Phys. **67**, 781 (1995).
- [9] J.N. Bahcall, M. Kamionkowski and A. Sirlin, Phys. Rev. D **51**, 6146 (1995).
- [10] J.N. Bahcall et al., Phys. Rev. D **54**, 411 (1996).
- [11] F.D. Stacey, *Physics of the Earth, 2nd edition*, John Wiley and Sons, London, New York, 1977.
- [12] R. Jeanloz, Annu. Rev. Earth Planet. Sci. **18**, 356 (1990).
- [13] A.D. Dziewonski and D.L. Anderson, Physics of the Earth and Planetary Interiors **25**, 297 (1981).

- [14] C.J. Allègre et al., *Earth and Planetary Science Letters* **134**, 515 (1995).
- [15] B. Bertotti and M. Maris, *Variabilitemporale del Flusso di Neutrini Solari in Esperimenti Sotterranei (Neutrino Flux Time Variability in Underground Experiments)*, reported in the Ph. D. thesis of M. Maris, Department of Theoretical and Nuclear Physics (D.F.N.T.), Pavia University, 1996, Italy.

Figure Captions

Figure 1. Recoil - e^- spectrum to be measured in the Super - Kamiokande experiment. Shown in the figure are the standard spectrum $\mathcal{S}_0(T_e)$ (upper solid line) and the one year average *Day* (long-dashed line), *Night* (short-dashed line), *Core* (lower solid line) and *Mantle* (dotted line) sample spectra in the case of a matter effect with parameters $\sin^2 2\theta_V = 0.01$ and $\Delta m^2 = 5 \times 10^{-5} \text{ eV}^2$ and for $Y_e = 0.467$. All spectra are normalized to the event rate in the Super - Kamiokandedetector, predicted in the reference solar model [8] for $T_{e,th} = 5 \text{ MeV}$

Figures 2.1 - 2.12. Recoil - e^- spectrum distortion $\mathcal{N}^s(T_e)$ (upper frame) and D-N asymmetry in the spectrum \mathcal{A}_{D-N}^s (lower frame) (see eqs. (4) and (5)) for the *Day* (long-dashed line), *Night* (short-dashed line), *Core* (solid line) and *Mantle* (dotted line) samples for $Y_e = 0.467$. The values of Δm^2 and $\sin^2 2\theta_V$ are indicated between the upper and the lower frames.

Figures 3a - 3c. Iso - (D-N) asymmetry contour plots for the one year average *Night* (a), *Core* (b) and *Mantle* (c) samples for the Super - Kamiokande detector. The solid (dash-dotted) lines in figures a and b correspond to $Y_e = 0.467$ (0.500). The dashed lines show the “conservative” MSW solution regions, while the dotted lines indicate the MSW solution regions obtained within the reference solar model [8].

Table I. Event Rates for the Super - Kamiokande Detector.

N.	$\sin^2 2\theta_V$	Δm^2	f_B	Event Rates $\mathcal{R}^s/\mathcal{R}_0$			
				<i>Day</i>	<i>Night</i>	<i>Core</i>	<i>Mantle</i>
1	0.0008	9e-6	0.4	0.8441	0.8434	0.8396	0.8440
2	0.0008	7e-6	0.4	0.8742	0.8724	0.8633	0.8739
3	0.0008	5e-6	0.4	0.9052	0.9018	0.8936	0.9032
4	0.0010	9e-5	0.4	0.2413	0.2413	0.2413	0.2413
5	0.0010	7e-6	0.4	0.8472	0.8451	0.8347	0.8469
6	0.0010	5e-6	0.4	0.8847	0.8807	0.8713	0.8823
7	0.0020	1e-5	0.5	0.6426	0.6421	0.6400	0.6425
8	0.0020	7e-6	0.5	0.7271	0.7245	0.7119	0.7266
9	0.0020	5e-6	0.5	0.7905	0.7849	0.7726	0.7870
10	0.0040	1e-5	1.0	0.4408	0.4414	0.4443	0.4410
11	0.0040	7e-6	0.7	0.5469	0.5467	0.5463	0.5468
12	0.0040	5e-6	0.7	0.6378	0.6341	0.6292	0.6349
13	0.0060	1e-5	1.5	0.3233	0.3256	0.3365	0.3239
14	0.0060	7e-6	1.0	0.4244	0.4289	0.4527	0.4251
15	0.0060	5e-6	0.7	0.5224	0.5249	0.5380	0.5228
16	0.0080	1e-5	1.5	0.2543	0.2584	0.2780	0.2552
17	0.0080	7e-6	1.5	0.3406	0.3511	0.4038	0.3424
18	0.0080	5e-6	1.0	0.4351	0.4464	0.4822	0.4404
19	0.0100	7e-6	1.5	0.2830	0.2997	0.3823	0.2860
20	0.0100	5e-6	1.0	0.3688	0.3901	0.4501	0.3802
21	0.0130	5e-6	1.5	0.2979	0.3349	0.4302	0.3192
22	0.3000	1.5e-5	2.0	0.2171	0.2417	0.2479	0.2407
23	0.3000	2e-5	2.0	0.2180	0.2354	0.2400	0.2346
24	0.3000	3e-5	2.0	0.2214	0.2322	0.2341	0.2319
25	0.3000	4e-5	2.0	0.2275	0.2351	0.2367	0.2349
26	0.4800	3e-5	1.5	0.2717	0.2883	0.2909	0.2879
27	0.4800	5e-5	1.5	0.2887	0.2975	0.2990	0.2972
28	0.5000	2e-5	1.5	0.2735	0.3007	0.3053	0.3000
29	0.5600	1e-5	1.5	0.2900	0.3678	0.4126	0.3604
30	0.6000	8e-5	1.0	0.3685	0.3738	0.3746	0.3736
31	0.7000	3e-5	1.0	0.3449	0.3682	0.3709	0.3677
32	0.7000	5e-5	1.0	0.3588	0.3711	0.3731	0.3708
33	0.7700	2e-5	1.0	0.3697	0.4082	0.4097	0.4079
34	0.8000	1.3e-4	0.7	0.4744	0.4771	0.4777	0.4770
35	0.9000	4e-5	0.7	0.4438	0.4644	0.4672	0.4639
36	0.9000	1e-4	0.7	0.4765	0.4820	0.4829	0.4819

The results correspond to $Y_e = 0.467$. The event rates \mathcal{R}^s and \mathcal{R}_0 (see eqs. (3) and (4)) were computed for $T_{e,th} = 5$ MeV. The factor f_B is the ratio of the value of the ${}^8\text{B}$ neutrino flux used in the MSW analysis and the flux predicted in the reference solar model [8]. The predicted event rates (in units of \mathcal{R}_0) are given by the product $f_B \mathcal{R}^s/\mathcal{R}_0$.

Table II. D - N Asymmetries for the Super - Kamiokande Detector.

N.	$\sin^2 2\theta_V$	Δm^2	f_B	$Y_e = 0.467$				$Y_e = 0.500$			
				$A_{D-N}^s \times 100$			$\frac{ A_{D-N}^C }{ A_{D-N}^N }$	$A_{D-N}^s \times 100$			$\frac{ A_{D-N}^C }{ A_{D-N}^N }$
				<i>Night</i>	<i>Core</i>	<i>Mantle</i>		<i>Night</i>	<i>Core</i>	<i>Mantle</i>	
1	0.0008	9.0e-6	0.4	-0.09	-0.54	-0.01	6.24	-0.12	-0.75	-0.01	6.25
2	0.0008	7.0e-6	0.4	-0.21	-1.26	-0.04	6.00	-0.22	-1.35	-0.04	6.14
3	0.0008	5.0e-6	0.4	-0.37	-1.29	-0.23	3.44	-0.35	-1.14	-0.23	3.26
4	0.0010	9.0e-5	0.4	3e-3	4e-3	3e-3	1.25	3e-3	4e-3	3e-3	1.33
5	0.0010	7.0e-6	0.4	-0.25	-1.50	-0.04	6.01	-0.26	-1.59	-0.04	6.12
6	0.0010	5.0e-6	0.4	-0.45	-1.52	-0.27	3.39	-0.43	-1.35	-0.27	3.14
7	0.0020	1.0e-5	0.5	-0.07	-0.41	-0.01	6.00	-0.10	-0.62	-0.01	6.20
8	0.0020	7.0e-6	0.5	-0.35	-2.10	-0.07	5.98	-0.36	-2.18	-0.07	6.06
9	0.0020	5.0e-6	0.5	-0.71	-2.30	-0.45	3.23	-0.67	-2.02	-0.45	3.01
10	0.0040	1.0e-5	1.0	0.15	0.79	0.04	5.42	0.22	1.28	0.04	5.82
11	0.0040	7.0e-6	0.7	-0.04	-0.12	-0.02	3.48	0.01	0.21	-0.02	21.00
12	0.0040	5.0e-6	0.7	-0.59	-1.36	-0.46	2.31	-0.56	-1.12	-0.47	2.00
13	0.0060	1.0e-5	1.5	0.72	3.98	0.17	5.56	1.05	6.20	0.17	5.90
14	0.0060	7.0e-6	1.0	1.06	6.46	0.17	6.13	1.26	7.60	0.17	6.03
15	0.0060	5.0e-6	0.7	0.47	2.93	0.06	6.19	0.46	2.82	0.06	6.13
16	0.0080	1.0e-5	1.5	1.63	8.93	0.37	5.47	2.36	13.59	0.37	5.76
17	0.0080	7.0e-6	1.5	3.04	17.00	0.53	5.59	3.39	19.10	0.53	5.63
18	0.0080	5.0e-6	1.0	2.55	10.26	1.22	4.02	2.44	9.54	1.22	3.91
19	0.0100	7.0e-6	1.5	5.72	29.85	1.05	5.22	6.28	32.85	1.05	5.23
20	0.0100	5.0e-6	1.0	5.60	19.84	3.03	3.54	5.36	18.38	3.03	3.43
21	0.0130	5.0e-6	1.5	11.69	36.33	6.89	3.11	11.21	33.72	6.89	3.01
22	0.3000	1.5e-5	2.0	10.73	13.25	10.31	1.24	11.03	15.29	10.30	1.39
23	0.3000	2.0e-5	2.0	7.64	9.60	7.31	1.26	7.79	10.66	7.31	1.37
24	0.3000	3.0e-5	2.0	4.74	5.54	4.61	1.17	4.78	5.85	4.61	1.22
25	0.3000	4.0e-5	2.0	3.29	3.93	3.18	1.20	3.31	4.07	3.19	1.23
26	0.4800	3.0e-5	1.5	5.95	6.81	5.81	1.15	5.99	7.08	5.81	1.18
27	0.4800	5.0e-5	1.5	2.98	3.50	2.89	1.17	2.99	3.57	2.89	1.19
28	0.5000	2.0e-5	1.5	9.48	10.97	9.24	1.16	9.60	11.79	9.23	1.23
29	0.5600	1.0e-5	1.5	23.65	34.9	21.64	1.48	27.50	40.77	25.11	1.48
30	0.6000	8.0e-5	1.0	1.42	1.64	1.38	1.15	1.42	1.65	1.38	1.16
31	0.7000	3.0e-5	1.0	6.54	7.26	6.41	1.11	6.56	7.43	6.41	1.13
32	0.7000	5.0e-5	1.0	3.37	3.90	3.29	1.16	3.38	3.95	3.29	1.17
33	0.7700	2.0e-5	1.0	9.89	10.27	9.83	1.04	9.94	10.59	9.83	1.07
34	0.8000	1.3e-4	0.7	0.57	0.69	0.55	1.21	0.57	0.69	0.55	1.21
35	0.9000	4.0e-5	0.7	4.53	5.12	4.42	1.13	4.53	5.17	4.42	1.14
36	0.9000	1.0e-4	0.7	1.15	1.33	1.13	1.15	1.15	1.33	1.13	1.16

Table III. Threshold Energy Dependence of the D - N Asymmetries ($Y_e = 0.467$).

N.	$\sin^2 2\theta_V$	Δm^2	f_B	$T_{e,th} = 5 \text{ MeV}$				$T_{e,th} = 7.5 \text{ MeV}$			
				$A_{D-N}^s \times 100$			$\frac{ A_{D-N}^C }{ A_{D-N}^N }$	$A_{D-N}^s \times 100$			$\frac{ A_{D-N}^C }{ A_{D-N}^N }$
				Night	Core	Mantle		Night	Core	Mantle	
1	0.0008	9.0e-6	0.4	-0.09	-0.54	-0.01	6.24	-0.13	-0.80	-0.02	6.30
2	0.0008	7.0e-6	0.4	-0.21	-1.26	-0.04	6.00	-0.29	-1.70	-0.06	5.91
3	0.0008	5.0e-6	0.4	-0.37	-1.29	-0.23	3.44	-0.43	-0.98	-0.34	2.30
4	0.0010	9.0e-5	0.4	3e-3	4e-3	3e-3	1.25	0.01	0.01	0.01	1.12
5	0.0010	7.0e-6	0.4	-0.25	-1.50	-0.04	6.01	-0.34	-2.02	-0.07	5.90
6	0.0010	5.0e-6	0.4	-0.45	-1.52	-0.27	3.39	-0.51	-1.18	-0.41	2.29
7	0.0020	1.0e-5	0.5	-0.07	-0.41	-0.01	6.00	-0.11	-0.65	-0.02	6.10
8	0.0020	7.0e-6	0.5	-0.35	-2.10	-0.07	5.98	-0.50	-2.92	-0.10	5.87
9	0.0020	5.0e-6	0.5	-0.71	-2.30	-0.45	3.23	-0.84	-1.86	-0.67	2.21
10	0.0040	1.0e-5	1.0	0.15	0.79	0.04	5.42	0.17	1.02	0.03	5.89
11	0.0040	7.0e-6	0.7	-0.04	-0.12	-0.02	3.48	-0.16	-0.79	-0.06	4.93
12	0.0040	5.0e-6	0.7	-0.59	-1.36	-0.46	2.31	-0.85	-1.61	-0.73	1.89
13	0.0060	1.0e-5	1.5	0.72	3.98	0.17	5.56	0.93	5.43	0.17	5.84
14	0.0060	7.0e-6	1.0	1.06	6.46	0.17	6.13	1.14	6.78	0.18	5.93
15	0.0060	5.0e-6	0.7	0.47	2.93	0.06	6.19	0.10	0.91	-0.04	9.15
16	0.0080	1.0e-5	1.5	1.63	8.93	0.37	5.47	2.17	12.30	0.39	5.66
17	0.0080	7.0e-6	1.5	3.04	17.00	0.53	5.59	3.44	18.87	0.64	5.48
18	0.0080	5.0e-6	1.0	2.55	10.26	1.22	4.02	2.08	5.62	1.48	2.70
19	0.0100	7.0e-6	1.5	5.72	29.85	1.05	5.22	6.65	33.61	1.33	5.06
20	0.0100	5.0e-6	1.0	5.60	19.84	3.03	3.54	5.09	12.23	3.86	2.40
21	0.0130	5.0e-6	1.5	11.69	36.33	6.89	3.11	11.34	24.62	8.95	2.17
22	0.3000	1.5e-5	2.0	10.73	13.25	10.31	1.24	12.61	15.40	12.14	1.22
23	0.3000	2.0e-5	2.0	7.64	9.60	7.31	1.26	9.03	11.99	8.53	1.33
24	0.3000	3.0e-5	2.0	4.74	5.54	4.61	1.17	5.57	6.45	5.42	1.16
25	0.3000	4.0e-5	2.0	3.29	3.93	3.18	1.20	3.99	4.78	3.86	1.20
26	0.4800	3.0e-5	1.5	5.95	6.81	5.81	1.15	6.95	7.85	6.80	1.13
27	0.4800	5.0e-5	1.5	2.98	3.50	2.89	1.17	3.64	4.27	3.53	1.17
28	0.5000	2.0e-5	1.5	9.48	10.97	9.24	1.16	11.07	13.36	10.69	1.21
29	0.5600	1.0e-5	1.5	23.65	34.9	21.64	1.48	28.78	46.48	25.45	1.62
30	0.6000	8.0e-5	1.0	1.42	1.64	1.38	1.15	1.85	2.13	1.81	1.15
31	0.7000	3.0e-5	1.0	6.54	7.26	6.41	1.11	7.56	8.26	7.44	1.09
32	0.7000	5.0e-5	1.0	3.37	3.90	3.29	1.16	4.05	4.67	3.95	1.15
33	0.7700	2.0e-5	1.0	9.89	10.27	9.83	1.04	11.34	11.91	11.25	1.05
34	0.8000	1.3e-4	0.7	0.57	0.69	0.55	1.21	0.78	0.93	0.75	1.20
35	0.9000	4.0e-5	0.7	4.53	5.12	4.42	1.13	5.32	6.02	5.20	1.13
36	0.9000	1.0e-4	0.7	1.15	1.33	1.13	1.15	1.46	1.63	1.43	1.12

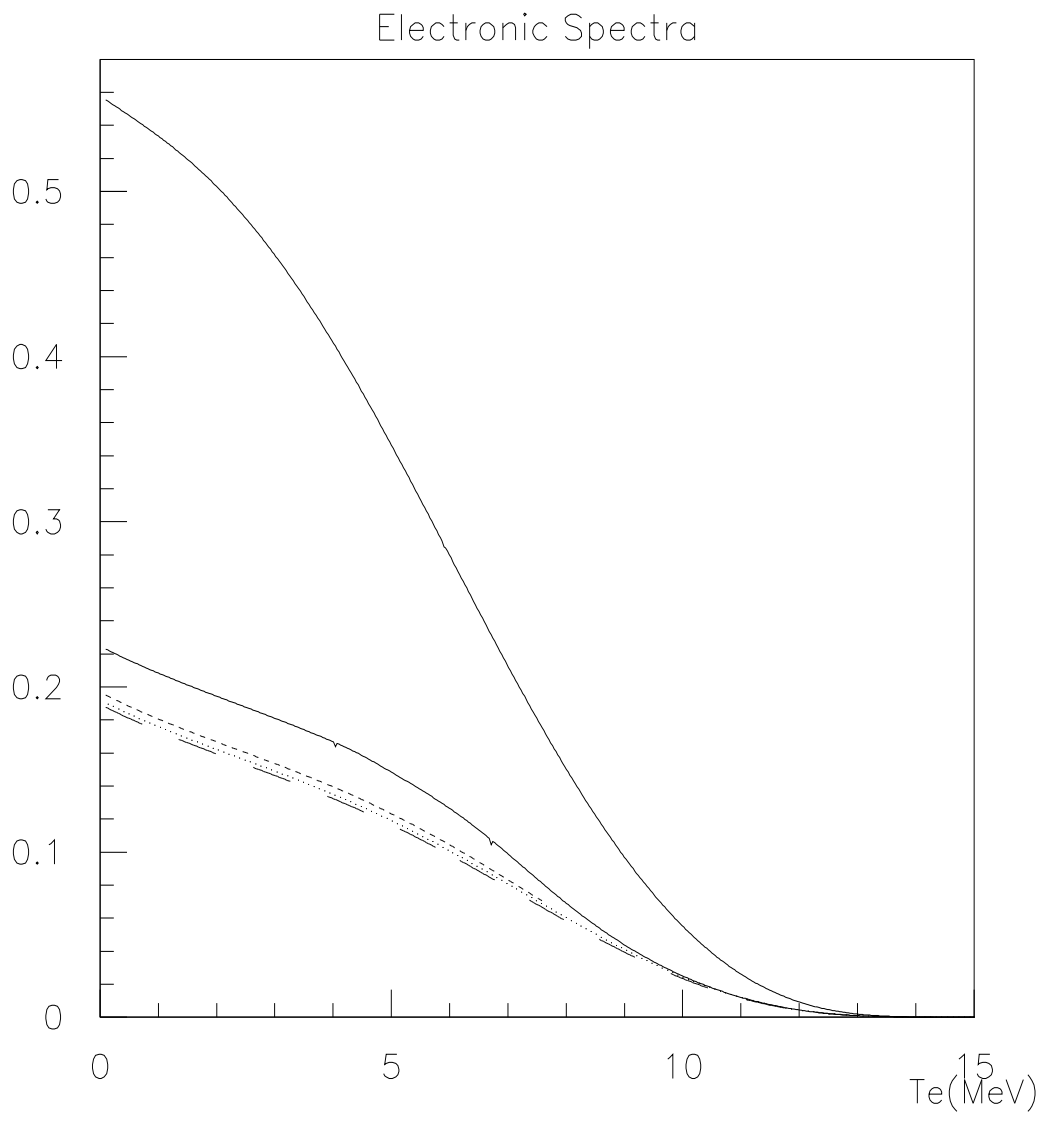


Figure 1

D-N Asymmetry for Full Night

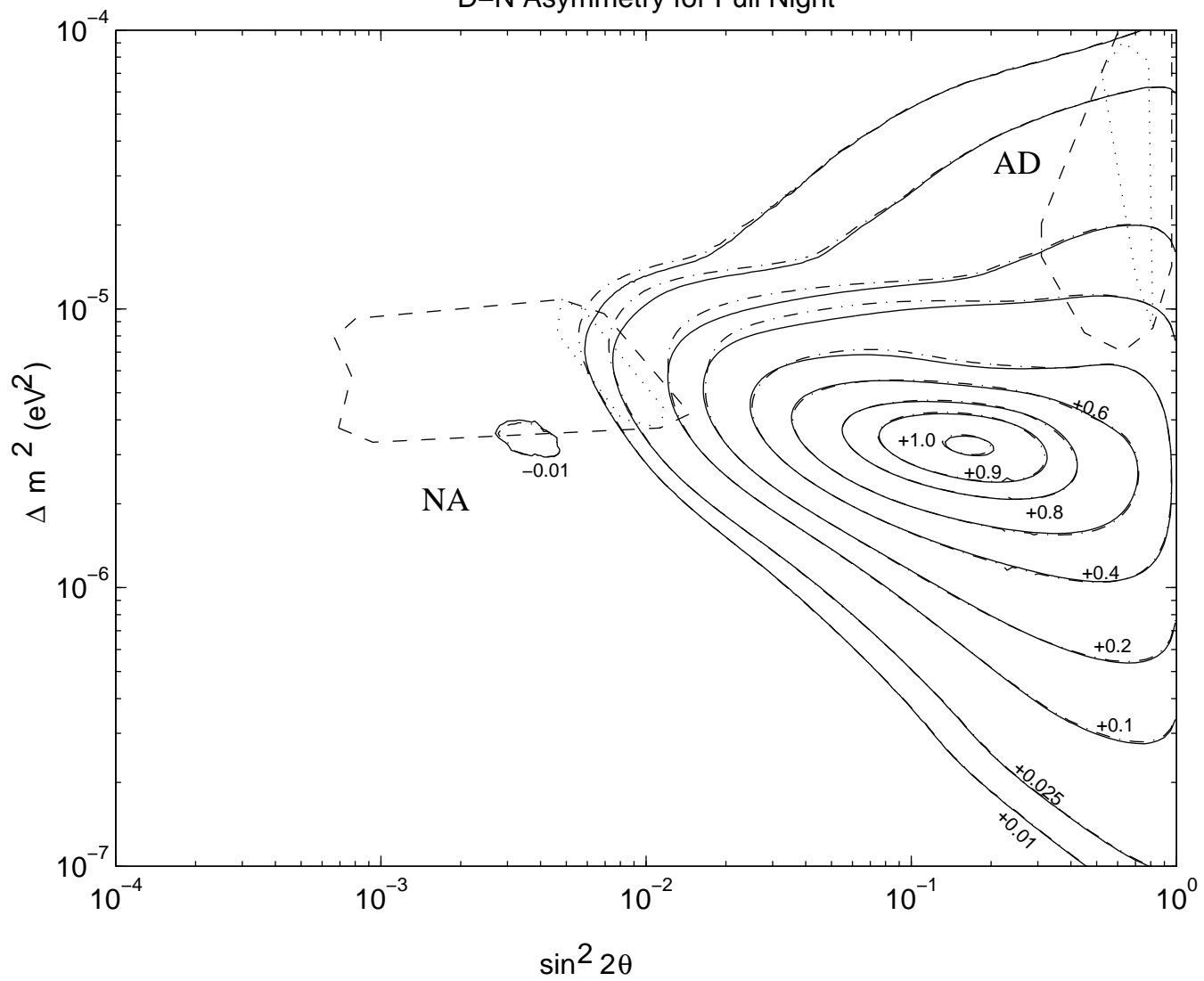


Figure 3.a

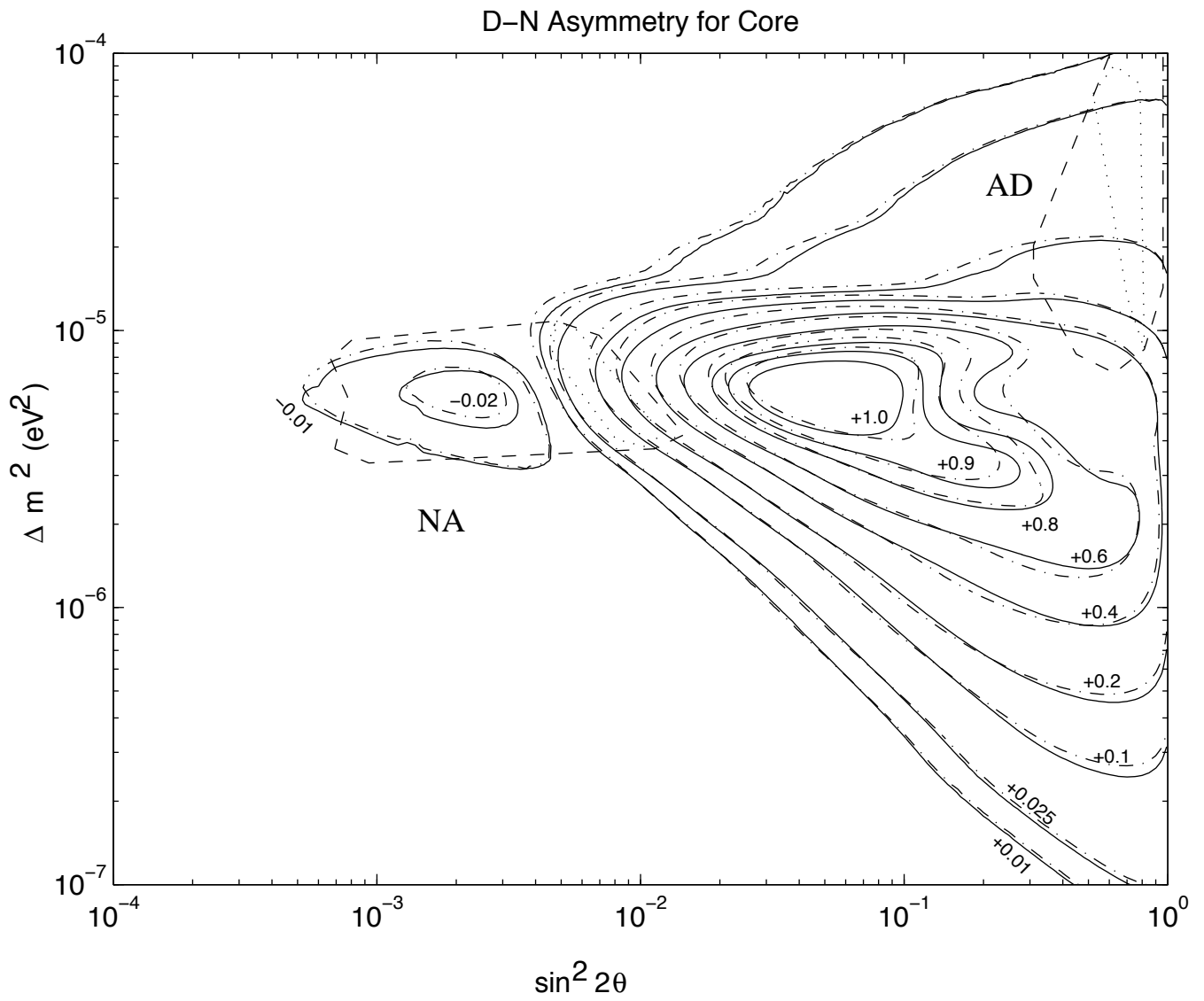


Figure 3.b

D-N Asymmetry for Mantle

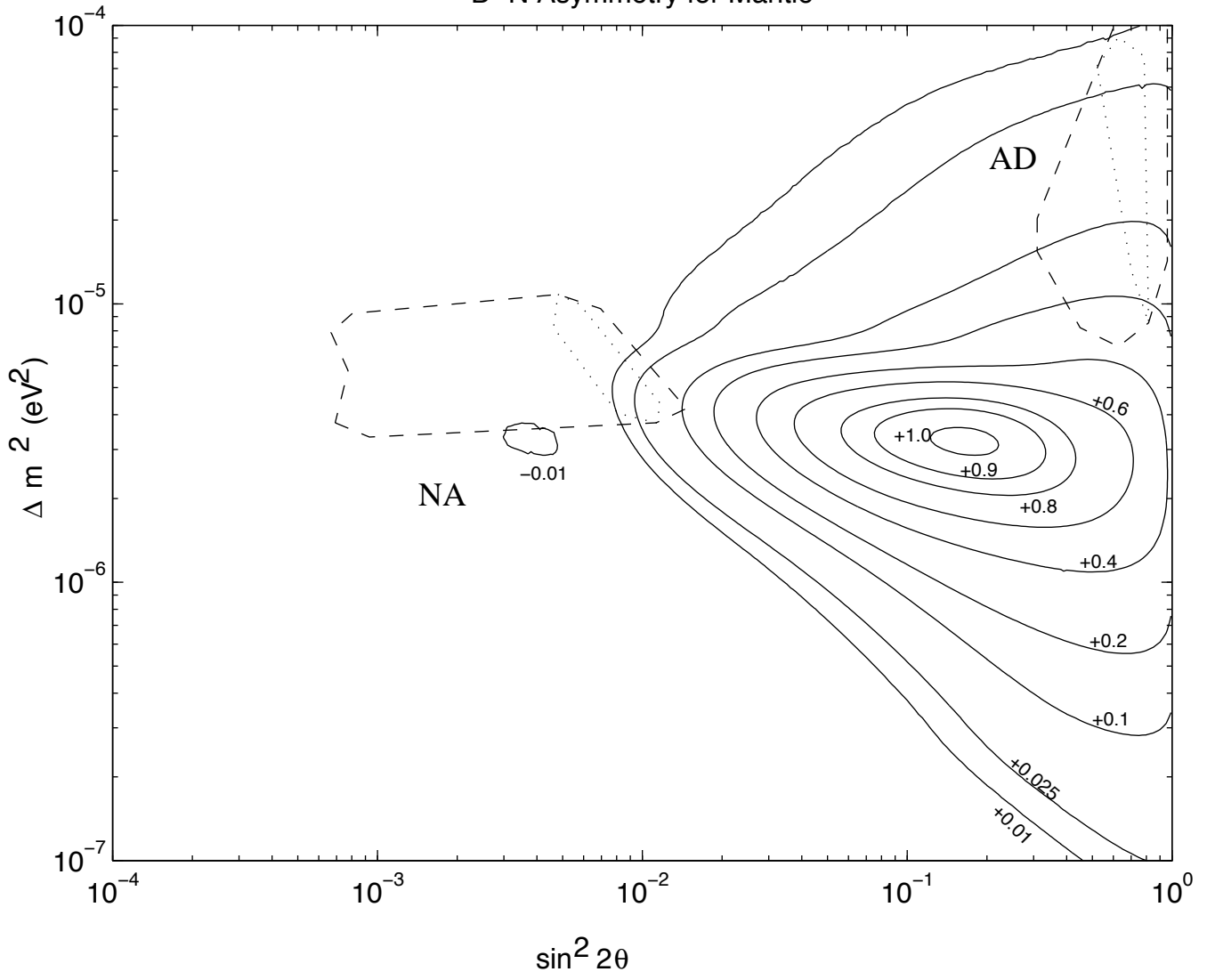


Figure 3.c

